

Generalized scaling of the transverse mass spectrum at the Relativistic Heavy-Ion Collider

Jürgen Schaffner-Bielich^a, Dmitri Kharzeev^b, Larry McLerran^b, and Raju Venugopalan^{a,b}

^a*RIKEN BNL Research Center, Brookhaven National Laboratory, Upton, NY 11973-5000, USA*

^b*Department of Physics, Brookhaven National Laboratory, Upton, NY 11973-5000, USA*

(February 22, 2019)

Abstract

We argue that the transverse mass spectra of identified hadrons as measured in gold-gold collisions at BNL's Relativistic Heavy-Ion Collider (RHIC) might follow a generalized scaling law. Such a scaling behavior is motivated by the idea of a Color Glass Condensate, or more generally, saturation of gluon density. In particular, we describe the shapes of transverse mass spectra as a function of centrality. This scaling of the transverse mass spectrum is shown to be consistent with previously observed scaling of multiplicity with centrality.

I. INTRODUCTION

In a previous work, two of us argued that the mean transverse momenta measured in relativistic heavy-ion collisions can be described by the intrinsic transverse momentum broadening seen at the Tevatron for $p\bar{p}$ collisions [1]. The mean transverse momenta of charged and identified hadrons increases universally with the square root of the multiplicity per unit transverse area for both $p\bar{p}$ and AA collisions. In addition, it has been shown that the total hadron multiplicity follows a scaling behavior motivated by the gluon saturation [2].

In this paper, we try to combine these two ideas in a consistent picture of transverse mass distributions of identified particles as a function of centrality. To do this, we apply theoretical ideas emerging in the Color Glass Condensate description of the high gluon density phase of QCD. Specifically, we describe the transverse momentum spectra using the recently measured data from BNL's Relativistic Heavy-Ion Collider (RHIC) for AuAu collisions at $\sqrt{s} = 130$ AGeV.

The theoretical motivation for such scaling relations is as follows. At very high energies, the number of partons (primarily gluons) in a nucleus grows very rapidly. When the occupation number of these partons is large, they saturate [3–5] and form a novel state of matter called a Color Glass Condensate (CGC) [2,6–11]. The CGC has a bulk scale Q_s ($\gg \Lambda_{QCD}$) which is the typical intrinsic transverse momentum of the saturated gluons in the nucleus. The CGC can be probed in deeply inelastic scattering [12,13], in photoproduction in peripheral heavy-ion collisions [14], in pA collisions [15,16] and in heavy-ion collisions [2,10,11].

II. GENERALIZED M_T -SCALING

A. Scaling Relations

Collisions of heavy-ions at high energies can be imagined as the collision of two sheets of colored glass, and a large multiplicity of gluons is produced. Since the occupation number of the gluons in each of the colliding nuclei is large, the problem can be treated classically [10]. The only dimensionful quantities available to describe the collision are a) the transverse area of the two colliding nuclei σ and b) the saturation scale Q_s^2 we mentioned previously, which is determined by the density of partons in the transverse plane. This saturation scale is a function of both energy and centrality. All dimensionful quantities can therefore be expressed in terms of powers of one or the other scale times non-perturbative functions of the dimensionless product of the two scales. The initial momentum distribution of produced gluons in high-energy collisions is then found to be given by the relation [11]

$$\frac{1}{\sigma} \frac{dN_g}{dy d^2p_t} = \frac{1}{\alpha_s(Q_s^2)} f_g \left(\frac{p_t^2}{Q_s^2} \right) . \quad (1)$$

Here, f_g is a universal, dimensionless function for the produced gluons which depends only on the ratio of the transverse momentum and the saturation momentum. Different energies or scales are described by the same function with a correspondingly changed saturation momentum Q_s .

Motivated by the above relation, we want to test in this paper how well these scaling relations describe the actual data, i.e. the momentum distribution of produced hadrons. Ab initio, it is not obvious that there is such a relation as hadrons are produced nonperturbatively at the deconfinement phase transition. There is also surely some transverse flow of the matter produced in these collisions and it is not clear to what degree this flow might distort the distributions produced early in the CGC.

We find that the transverse momentum distributions of identified particles are well described as a function only of the transverse mass $m_t = \sqrt{m_h^2 + p_t^2}$. This appears to be a good approximation so long as we are not too close to the mass of the particle in question. (At small values of p_t we expect flow effects to be important which will invalidate this simple m_t scaling form of the distributions.) We therefore parameterize the transverse momentum spectra as

$$\frac{1}{\sigma} \frac{dN_h}{dy d^2m_t} = \frac{1}{\alpha_s(p_s)} \kappa_h \cdot f \left(\frac{m_t}{p_s} \right) . \quad (2)$$

The universal function f depends only on m_t , and incorporates m_t -scaling. The constant κ_h reflects the difference in abundances of various species of particles, and is of order one for the particles which we consider. We take it to be independent of p_s . The momentum p_s as well as σ are parameters which are determined by the energy and centrality of the collision. The momentum p_s is assumed to have the same energy and centrality dependence as the saturation momentum Q_s . Also, the function f has to be extracted from the data. But once the universal function f is fixed for one data set, it should describe the other data by rescaling the parameters p_s and σ . Hence, the scaling relation implies that there is one and only one function which describes high-energy collisions at various centralities, energy and system size. This picture can certainly be valid only in some range of these parameters. How well scaling works for data from relativistic heavy-ion collisions is the purpose of this investigation.

B. Comparison with RHIC Data

We turn now to a more detailed discussion of the transverse momentum distribution focusing on identified hadron spectra as measured recently at RHIC in AuAu collisions with $\sqrt{s} = 130$ AGeV [17–20]. Note that in relation (2) all hadrons are described by only one function of the transverse mass $m_t = \sqrt{m_0^2 + p_t^2}$. The transverse mass is just the total transverse kinetic energy carried by that hadron. Plotting the transverse mass spectra for identified hadrons as a function of m_t (not as a function of $m_t - m_0$) should then result in one single curve. This idea is not particularly new. It is similar to the m_t -scaling behavior put forward by Hagedorn for pp collisions in his statistical model [21]. The universal function in the Hagedorn model is then a Bose-Einstein or Fermi-Dirac distribution and depends on one parameter, the slope parameter T_{slope} . Contrary to this picture, we approach the problem in reverse and try to determine the universal function from the experimental data.

The transverse momentum spectra of pions, kaons, protons and antiprotons have been reported by the PHENIX collaboration at RHIC to quite large transverse momenta p_t [18]. For the first time in hadronic collisions, one sees that the protons and antiprotons seem to

be more abundant at higher transverse momentum $p_t > 2$ GeV than pions. The slope of the transverse momentum spectra for protons and antiprotons is apparently much larger than that of the pions, so that the nucleon spectra overshoots the pion spectra at some $p_t > 2$ GeV.

The scaling relation (2) can now be tested by plotting the transverse mass spectra. Figure 1 shows the preliminary minimum bias data of the PHENIX collaboration for charged pions, kaons, protons and antiprotons [18] and for neutral pions [19] as a function of m_t (not p_t). As one can see from Fig. 1, the data points for all hadrons seem to follow one curve over several orders of magnitude for a broad range of transverse mass. The neutral pion data is on top of the antiproton data within the error bars. But one notices also, that the curves for kaons and protons are shifted downwards and upwards, respectively. These are effects due to quantum numbers (strangeness and baryon number) which are not taken into account in the scaling relation. The production of strange particles is suppressed due to the strange quark mass, while the number of protons is enhanced due to the initial baryon number excess coming from the two colliding nuclei. Interestingly the proton-antiproton pair production seems to be not suppressed but kaon production is relative to pion production. We note that these changes are moderate, they shift the curves of the kaons down by about a factor two while shifting the proton curve up by about a factor two from the universal curve. Shifting the kaon and the proton spectra by these factors results in Fig. 2. Now all the data points are lying on one curve. It tells us that the shape of the spectra for the same value of m_t are equal for pions, kaons, and nucleons. (Oftentimes a slope parameter is extracted to characterize spectra. This is extracted from the spectra close to the mass threshold, i.e. at $m_t = m_h$. The larger the mass of the hadron m_h the larger will be its slope parameter T_{slope} , as the slope of the transverse mass spectra is increasing with m_t . We can read from Fig. 2, that this effect will also continue for heavier particles but it is less pronounced as the slope of the curve levels off.) If scaling works for all particles, the transverse mass distribution of hyperons will then follow also the same universal m_t -curve of Fig. 2 modulo shape independent effects from baryon and strangeness number conservation which affect only the overall normalization of the distribution.

Being more quantitative, the transverse mass spectra of Fig. 2 can be fitted by a power law of the form $(1 + m_t/p_s)^{-n}$ with the parameters $n = 16.3$ and $p_s = 2.71$ GeV. We remark that the values for n and p_s are strongly correlated, fits with different values for p_s and properly adjusted n gives an equally good fit to the data points. The values for n and p_s are constrained in such a way that they get about the same mean transverse mass of

$$\langle m_t \rangle = \frac{2p_s}{n - 3} \quad (3)$$

for each fit. Let us define now the local slope as

$$-\frac{1}{T_{\text{slope}}} = \frac{d}{dm_t} \ln(f(m_t/p_s)) \quad . \quad (4)$$

Then we find that the local slope parameter for a power-law distribution in m_t is given by

$$T_{\text{slope}} = \frac{p_s}{n} + \frac{1}{n} m_t \quad . \quad (5)$$

i.e. a constant term plus a term linear in the transverse mass. The constant is closely related to the mean transverse mass. The correction term proportional to the transverse mass originates from the non-exponential behavior of the power-law distribution which enhances the high- m_t part of the distribution. With the fitted parameters given above, we find the following slope parameters for various hadrons at $m_t = m_h$: 175 MeV (π), 196 MeV (K), 224 MeV (p), 235 MeV (Λ), 247 MeV (Ξ). The actual measured values for π , K and nucleons are higher [18] as the experimental fits are taken around 0.5 GeV above the threshold. Hence, the apparently different slopes for hadrons can be also explained by a generalized m_t -scaling of the transverse mass spectra. Note, that the relation (5) is similar to the one derived for radial flow of non-relativistic particles $T_{\text{slope}} = T_0 + 0.5\beta^2 \cdot m_h$ [22]. In pp collisions, the value for p_s is smaller than in AA collisions, so that the deviations from an exponential shape of the transverse mass distribution are less pronounced. Therefore, one recovers in pp collisions the traditional m_t -scaling behavior of Hagedorn's statistical model [21] with about similar slope parameters for all hadrons. We will discuss the centrality dependence below in more detail.

We remark, that the universal m_t -scaling seen in Fig. 1 does not rule out radial flow. At large momenta, also the hydro picture predicts a universal curve for all hadrons. A clear indication of radial flow would now be a deviation from the m_t -scaling curve. It is likely to expect these deviations in the low momentum part of the distribution, as this part is easiest to thermalize. The effect of radial flow should be especially pronounced for heavier hadrons. STAR measures at even lower p_t than PHENIX and reports a larger slope parameter for antiprotons than PHENIX [20]. This experimental finding can not be explained by generalized m_t -scaling. The flatter distribution at small m_t close to m_h compared to larger m_t can be well described in hydrodynamical models with collective transverse flow [23,24]. In general, radial flow implies a violation of m_t scaling, as the transverse momentum distribution depends then on both, on m_t and on p_t .

In reality, we expect that there should be radial flow effects in heavy ion collisions. These should show up in a relatively unambiguous way as the deviations from m_t scaling for m_t near threshold. What we try to describe in this paper are the gross features of the data for m_t far from threshold. In this region, it is harder to justify a hydrodynamic description. It might nevertheless turn out that the scaling we observe in this paper can also be explained by radial flow even at large m_t . The relations which we derive in this paper depend upon a saturation momenta and the consistency of the picture we present is simple within the Color Glass Condensate picture, but it may turn out for reasons which we do not understand that radial flow preserves these simple patterns. For example, this might be plausible if the flow sets in very early in the collision. It might also turn out that the patterns we observe have some as yet undiscovered interpretation. The scaling relations we present nevertheless would remain as a simple phenomenological description of the data.

Finally, we note that the universal m_t -scaling for hadrons in heavy-ion collisions has been also observed at lower bombarding energies at CERN's SPS [25,26] but it has not been discussed in detail. In particular, no interpretation in terms of scaling has been given.

III. SCALING WITH CENTRALITY

The scaling relation (2) predicts more than the universal curve for the transverse mass spectra. As it should be valid for all centralities, the transverse mass spectra should scale for each centrality class. Moreover, there is only one scaling function and the transverse mass spectra for different centralities can then be rescaled into each other by properly choosing the transverse area σ and the momentum p_s for each centrality bin.

The first statement is probed in Fig. 3 which shows the preliminary m_t -spectra of PHENIX for negatively charged pions and antiprotons for different centralities [18]. Indeed, it seems that there is a universal function for each centrality bin, even for the most peripheral one, which describes the pion and antiproton spectra simultaneously. The form of the curves looks similar for the various centralities, too.

To check that the m_t distribution is universal, we rescale the data points in absolute normalization and in transverse mass:

$$\frac{1}{\sigma} \frac{dN_h}{dyd^2m_t} \rightarrow \frac{1}{\lambda} \frac{1}{\sigma} \frac{dN_h}{dyd^2m_t} \quad \text{and} \quad m_t \rightarrow \frac{m_t}{\lambda'} \quad (6)$$

so that the data points for all centralities are lying on top of each other. We choose the most central bin as a reference curve. The scaling parameters λ and λ' are extracted for each centrality bin. The scaling parameter λ is just $\sigma/\alpha_s(p_s)$ for a given centrality relative to the value for the most central bin. The parameter λ' is the momentum p_s for a given centrality bin divided by the one for the most central bin. Technically, we use the p_t -spectra of charged particles as measured by the PHENIX collaboration [17] to fix the scaling parameters λ and λ' for each centrality bin as the data has much better statistics. Then we use those parameters to rescale the m_t distributions.

Fig. 4 shows the rescaled version of the transverse mass spectra for all centralities. The data points for all centralities are now lying on top of each other, i.e. scaling works reasonably well also for the centrality dependence of the m_t -spectra. Accordingly, also the charged particle p_t spectra then can be rescaled for each centrality cut. There seem to be deviations from scaling at large m_t in Fig. 4 as that the more central bins are suppressed relative to the peripheral ones. But within the error bars it is difficult to make a more definite conclusion. We see a similar trend at high p_t for the rescaled charged particle spectra, but again within the error bars it is hard to draw a conclusion.

The rescaling factors, i.e. the change of $\sigma/\alpha(p_s)$ and p_s as a function of centrality, are expected to follow the transverse area of the two colliding nuclei and the saturation momentum of the CGC for given impact parameter b . In the following we will check, if this is the case.

A. Scaling of the Transverse Area

The fitted scaling factor $\sigma/\alpha_s(p_s)$ for the different centrality bins are plotted in Fig. 5 versus the number of participants N_{part} . We take the number of participants as reported by the PHENIX collaboration in [27] for their centrality cuts. The scaling factors are given relative to the one for the most central bin at $N_{\text{part}} = 347$.

One sees from the figure, that the fitted scaling factors seems to have a more linear dependence on N_{part} than to follow the curve for a transverse area $A \sim N_{\text{part}}^{2/3}$. Nevertheless, there is correction factor coming from $\alpha_s(p_s)$. The quantity α_s is taken as $\alpha_s^{-1} \sim \ln(Q_s^2/\Lambda_{\text{QCD}}^2)$ and the saturation momentum is dependent on the number of participants N_{part} [2]. The factor α_s induces then a logarithmic correction to the scaling factor. The scaling factor should then follow a curve proportional to the transverse area A divided by α_s which is of the form $N_{\text{part}}^{2/3} \ln(N_{\text{part}})$. The corresponding curve is shown in Fig. 5 by the solid line and follows now very closely the extracted values for the scaling factor.

B. Scaling of the Transverse Momentum

The second scaling factor, p_s^2 , as extracted from the data is shown in Fig. 6. Again, the factors are normalized to the one for the most central bin. The centrality dependence of p_s^2 is quite weak for moderate to large number of participants but falls off for peripheral collisions. The fitted values of p_s^2 are compared with the expected behavior for the saturation momentum $Q_s^2 \sim N_{\text{part}}^{1/3}$ in the figure. It is seen, that p_s changes less rapidly with centrality than $N_{\text{part}}^{1/3}$. The reason is that the gluon densities at hand are still too small to reach this behavior fully. Fits of the form $c + N_{\text{part}}^{1/3}$ describe the centrality dependence of p_s much better (see figure). Hence, as p_s increases it appears to be tending towards the scaling with $N_{\text{part}}^{1/3}$.

Let us compare p_s to the mean transverse momentum defined by

$$\langle p_t \rangle = \frac{p_s^3 \cdot \int_{m_h/p_s}^{\infty} d^2x \sqrt{x^2 - (m_h/p_s)^2} f(x)}{p_s^2 \cdot \int_{m_h/p_s}^{\infty} d^2x f(x)} = p_s \cdot P\left(\frac{m_h}{p_s}\right) , \quad (7)$$

where m_h is the vacuum mass of the identified hadron and P is some function of the ratio of the hadron mass and the scaling momentum. The momentum p_s is proportional to the mean p_t . In the limit $N_{\text{part}} \rightarrow 2$ one should recover the mean p_t and its corresponding momentum p_s of pp collisions. The constant seen in the fit of p_s with N_{part} then stands for that finite mean p_t (or p_s) already present in pp collisions. Note, that p_s is not directly identical with the mean p_t but differs by the factor P . As this factor P depends on the vacuum mass of the hadron, the mean p_t for each hadron follows a different behavior with centrality which depends on the ratio of its vacuum mass to the momentum p_s in a nontrivial way.

The weak centrality dependence of p_s is compatible with the small change of the mean p_t with N_{part} seen at RHIC [18,28]. The mean p_t for charged particles measured in $p\bar{p}$ collisions at $\sqrt{s} = 200$ GeV has been measured by the UA1 collaboration to be $\langle p_t \rangle = 392 \pm 3$ MeV [29]. The energy dependence of the mean p_t for $p\bar{p}$ collisions is known to be quite weak. STAR reports preliminarily that $\langle p_t \rangle = 508 \pm 12$ MeV for central AuAu collisions at $\sqrt{s} = 130$ GeV [20,28]. So, the ratio of mean p_t squared for $N_{\text{part}} \rightarrow 2$ to the value for central AuAu collisions, i.e. the value for p_s^2 at $N_{\text{part}} = 2$, is calculated to be 0.60 which is in agreement with the results of Fig. 6.

The centrality dependence for p_s can be compared to the measured transverse energy per charged particle by the PHENIX collaboration [30] which is approximately proportional to the mean transverse momentum. The data points are flat from the most central bin down

to $N_{\text{part}} \sim 76$. The extracted values for p_s in Fig. 6 follow closely this constant dependence on centrality for these values of N_{part} .

C. Multiplicity

We can cross-check our scaling relations by computing the centrality dependence of the charged multiplicity. Integrating eq. (2) over the transverse mass gives the multiplicity

$$\frac{dN}{dy} = \frac{\sigma}{\alpha_s} p_s^2 \cdot \kappa_h \int_{m_h/p_s}^{\infty} d^2x f(x) = \frac{\sigma p_s^2}{\alpha_s} \cdot \kappa_h F\left(\frac{m_h}{p_s}\right) , \quad (8)$$

The dependence of the multiplicity on the scaling factors is analogous to the multiplicity dependence of initially produced gluons in the CGC (see e.g. [2] and references therein):

$$\frac{dN}{dy} \sim \frac{\sigma Q_s^2}{\alpha_s} , \quad (9)$$

except for the last factor κ_h which takes into account normalization effects associated with different species of particles. These are small corrections to these formula, as e.g. the kaon spectra is lying about a factor two below the universal curve in m_t (see our discussion of Fig. 4). Neglecting the dependence of the shift from rapidity y to pseudo-rapidity η on centrality, the charged multiplicity density reads

$$\frac{1}{N_{\text{part}}} \frac{dN}{d\eta} \sim \frac{\sigma p_s^2}{\alpha_s N_{\text{part}}} \left[\kappa_\pi F\left(\frac{m_\pi}{p_s}\right) + \kappa_K F\left(\frac{m_K}{p_s}\right) + \kappa_p F\left(\frac{m_p}{p_s}\right) + \dots \right] . \quad (10)$$

If we take the universal function f to be a power law in the transverse mass:

$$f\left(\frac{m_t}{p_s}\right) \sim \left(1 + \left(\frac{m_t}{p_s}\right)\right)^{-n} \quad (11)$$

then it can be analytically integrated to get

$$F\left(\frac{m_h}{p_s}\right) \sim \frac{1}{(n-2)(n-1)} \left(\frac{p_s}{m_h + p_s}\right)^{n-1} \left(1 + (n-1)\frac{m_h}{p_s}\right) . \quad (12)$$

Indeed, one can perform a power law fit to the transverse mass spectra of the preliminary PHENIX data of the most central bin of Fig. 4 with $n = 11.8$ and $p_s = 1.65$ GeV. We can now compute the charged multiplicity from the two scaling factors and the power law function for the most central bin.

Quantitatively, the factor σ/α_s grows approximately like N_{part} (see Fig. 5) and p_s^2 grows like $c + N_{\text{part}}^{1/3}$ (see Fig. 6), so that finally we recover

$$\frac{1}{N_{\text{part}}} \frac{dN}{d\eta} \sim \text{const.} + N_{\text{part}}^{1/3} . \quad (13)$$

This form is the one expected from the eikonal approach with a constant contribution from soft scatterings and a term growing with $N_{\text{part}}^{1/3}$ due to hard scatterings [2]. This form can

be motivated by noting that at large N_{part} it has a form consistent with our expectations concerning saturation. At low N_{part} , the constant reflects non-perturbative physics, perhaps associated with a vacuum gluon condensate [31,32]. The form above is the simplest formula which interpolates between these limits. That the dependence of the charged multiplicity on N_{part} comes out correctly is nontrivial. The multiplicity of particles is dominated by the contributions from small p_t where there it is possible to have deviations from the universal function due to resonance decays. As it turns out this does not seem to be the case qualitatively.

IV. TRANSVERSE MOMENTUM BROADENING REVISITED

The eqs. (7) and (10) give a relation between the mean transverse momentum and the charged multiplicity:

$$\langle p_t \rangle^2 \sim \alpha_s P^2 (m_h/p_s) \cdot \frac{1}{\sigma} \frac{dN}{d\eta} . \quad (14)$$

Except for the factor $\alpha_s P^2$, this is the relation as studied in [1]. The mean momentum squared increases as the charged multiplicity per transverse area. This has been found to be in good agreement with the $p\bar{p}$ data from the Tevatron and the heavy-ion data from the SPS [1]. We expect a similar behavior at RHIC from scaling arguments. Compared to the previous work [1], we are now in the position to explain in more detail the effects of p_t broadening, i.e. that the mean p_t rises more rapidly for more massive particles compared to the purely kinematic behavior as seen in $p\bar{p}$ collisions at the Tevatron [34–36]. The mass dependent factor $P(m_h/p_s)$ gives a different steepness in the increase of mean p_t squared for different hadrons, so that pions, kaons and nucleons have a different slope. As $P(m_h/p_s)$ increases with hadron mass m_h , the slope will be larger for more massive particles. If the function f is of exponential form, $f \sim \exp(-m_t/T)$, then the mean p_t is given by

$$\langle p_t \rangle = T \left(\frac{\pi m_h}{2T} \right)^{1/2} \frac{K_2(m_h/T)}{K_{3/2}(m_h/T)} . \quad (15)$$

For heavy particles, $m_h \ll T$, one gets $\langle p_t \rangle^2 \sim \pi/2m_h T$ which is besides a small correction factor just the purely kinematic factor $2m_h T$ for non-relativistic particles.

We show in Fig. 6 as a function of centrality the PHENIX data on the transverse energy per charged particle E_T/N_c [30]. The data has large systematic errors, and taken alone would provide no evidence of p_t broadening. The larger errors on this data nevertheless allow for consistency with the data on identified particle spectra (note that one has to compare the data points to p_s while we are plotting p_s^2 in the figure, which will bring the points for p_s closer to the data). The STAR data on mean p_t for charged particles shows a centrality dependence which appears consistent with our analysis [20,28].

ACKNOWLEDGMENTS

We thank Barbara Jacak, Julia Velkovska, and Nu Xu for many helpful discussions. J.S.B. acknowledges RIKEN, BNL, and the U.S. Department of Energy for providing the

facilities essential for the completion of this work. This manuscript has been authorized with the U.S. Department of Energy under Contract No. DE-AC02-98CH10886.

REFERENCES

- [1] L. McLerran and J. Schaffner-Bielich, Phys. Lett. B **514**, 29 (2001).
- [2] D. Kharzeev and M. Nardi, Phys. Lett. B **507**, 121 (2001); D. Kharzeev and E. Levin, nucl-th/0108006.
- [3] L. V. Gribov, E. M. Levin, and M. G. Ryskin, Phys. Rep. **100**, 1 (1983).
- [4] A. H. Mueller and J. W. Qiu, Nucl. Phys. B **268**, 427 (1986).
- [5] J. P. Blaizot and A. H. Mueller, Nucl. Phys. B **289**, 847 (1987).
- [6] L. McLerran and R. Venugopalan, Phys. Rev. D **49**, 2233 (1994); *ibid* 3352 (1994); *ibid* **50**, 2225 (1994); Y. Kovchegov, Phys. Rev. D **54**, 5463 (1996).
- [7] Y. V. Kovchegov, Phys. Rev. D **54**, 5463 (1996).
- [8] J. Jalilian-Marian, A. Kovner, L. McLerran, and H. Weigert, Phys. Rev. D **55**, 5414 (1997); J. Jalilian-Marian, A. Kovner, A. Leonidov, and H. Weigert, Nucl. Phys. B **504**, 415 (1997); Phys. Rev. D **59**, 014014 (1999).
- [9] E. Iancu, A. Leonidov, and L. McLerran, hep-ph/0011241 (2000).
- [10] A. Kovner, L. McLerran, and H. Weigert, Phys. Rev. D **52**, 6231 (1995); *ibid* 3809 (1995).
- [11] A. Krasnitz and R. Venugopalan, Phys. Rev. Lett. **86**, 1717 (2001); *ibid.*, **84**, 4309 (2000); Nucl. Phys. B **557**, 237 (1999); W. Pöschl and B. Müller, Comput. Phys. Commun. **125**, 282 (2000).
- [12] L. McLerran and R. Venugopalan, Phys. Rev. D **59**, 094002 (1999).
- [13] Y. V. Kovchegov and L. McLerran, Phys. Rev. D **60**, 054025 (1999) [Erratum: *ibid.* **62**, 019901 (1999)].
- [14] F. Gelis and A. Peshier, hep-ph/0107142 (2001).
- [15] Y. V. Kovchegov and A. H. Mueller, Nucl. Phys. B **529**, 451 (1998).
- [16] A. Dumitru and L. McLerran, hep-ph/0105268 (2001).
- [17] W. A. Zajc *et al.* [PHENIX Collaboration], nucl-ex/0106001 (2001).
- [18] J. Velkovska [PHENIX collaboration], nucl-ex/0105012 (2001) and private communication.
- [19] G. David [PHENIX collaboration], talk presented at Quark Matter 2001, January 15-20, 2001, Stony Brook, New York (see <http://www.rhic.bnl.gov/qm2001>); hep-ex/0105015 (2001) and private communication.
- [20] M. Calderon and J. Harris [STAR collaboration], talks presented at Quark Matter 2001, Stony Brook, New York.
- [21] R. Hagedorn, Nuovo Cim. Suppl. **3** (1965) 147; *ibid* **6**, 169 (1968).
- [22] T. Csörgő and B. Lörstad, Phys. Rev. C **54**, 1390 (1996); R. Scheibl and U. Heinz, Phys. Rev. C **59**, 1585 (1999).
- [23] P. Huovinen, P. F. Kolb, U. Heinz, P. V. Ruuskanen and S. A. Voloshin, Phys. Lett. B **503**, 58 (2001).
- [24] D. K. Srivastava, nucl-th/0104056 (2001).
- [25] K. S. Lee, U. Heinz and E. Schnedermann, Z. Phys. C **48**, 525 (1990).
- [26] Nu Xu, unpublished notes (1996) and private communication.
- [27] K. Adcox *et al.* [PHENIX Collaboration], Phys. Rev. Lett. **86**, 3500 (2001).
- [28] Zhangbu Xu [STAR collaboration], talk given at the RHIC/INT workshop on Ultra-relativistic Heavy Ion Collisions in the RHIC era, May 31 - June 2, 2001, Lawrence

Berkeley National Laboratory, Berkeley, California (see <http://www-nsdth.lbl.gov/rhic-int-2001/talks/Xu.pdf>).

- [29] C. Albajar *et al.* [UA1 Collaboration], Nucl. Phys. B **335**, 261 (1990).
- [30] K. Adcox *et al.* [PHENIX Collaboration], Phys. Rev. Lett. **87**, 052301 (2001); Alexander Bazilevsky, private communication.
- [31] D. Kharzeev and E. Levin, Nucl. Phys. B **578**, 351 (2000).
- [32] D. E. Kharzeev, Y. V. Kovchegov and E. Levin, Nucl. Phys. A **690**, 621 (2001); hep-ph/0106248 (2001); M. A. Nowak, E. V. Shuryak and I. Zahed, Phys. Rev. D **64**, 034008 (2001).
- [33] C. Adler *et al.* [STAR Collaboration], Phys. Rev. Lett. **86**, 4778 (2001).
- [34] T. Alexopoulos *et al.* [E735 collaboration], Phys. Rev. Lett. **60**, 1622 (1988).
- [35] T. Alexopoulos *et al.* [E735 collaboration], Phys. Rev. Lett. **64**, 991 (1990).
- [36] T. Alexopoulos *et al.* [E735 collaboration], Phys. Rev. D **48**, 984 (1993).

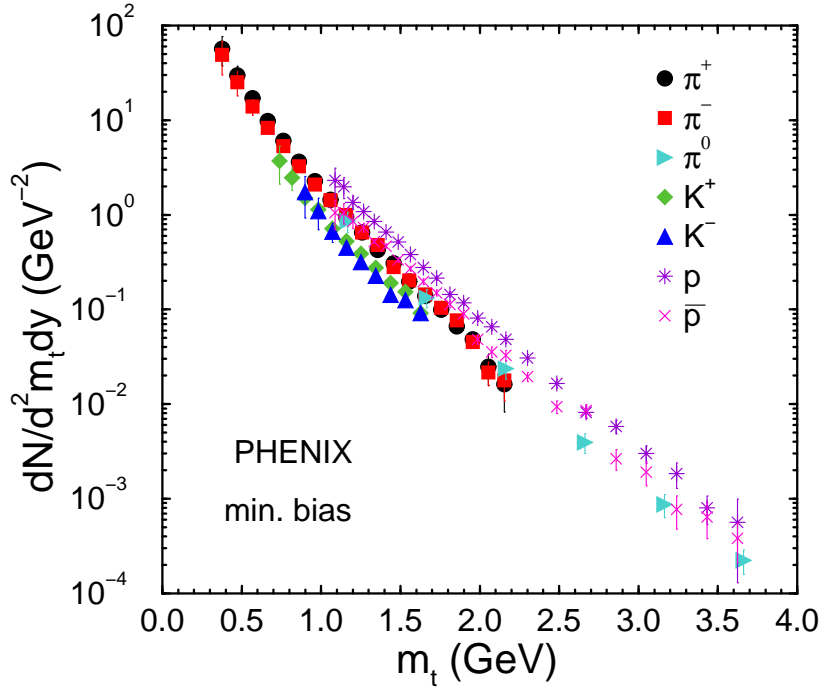


FIG. 1. Transverse mass spectra of identified hadrons for minimum bias gold-gold collisions as measured for $\sqrt{s} = 130$ AGeV at RHIC (data taken from [18,19]).

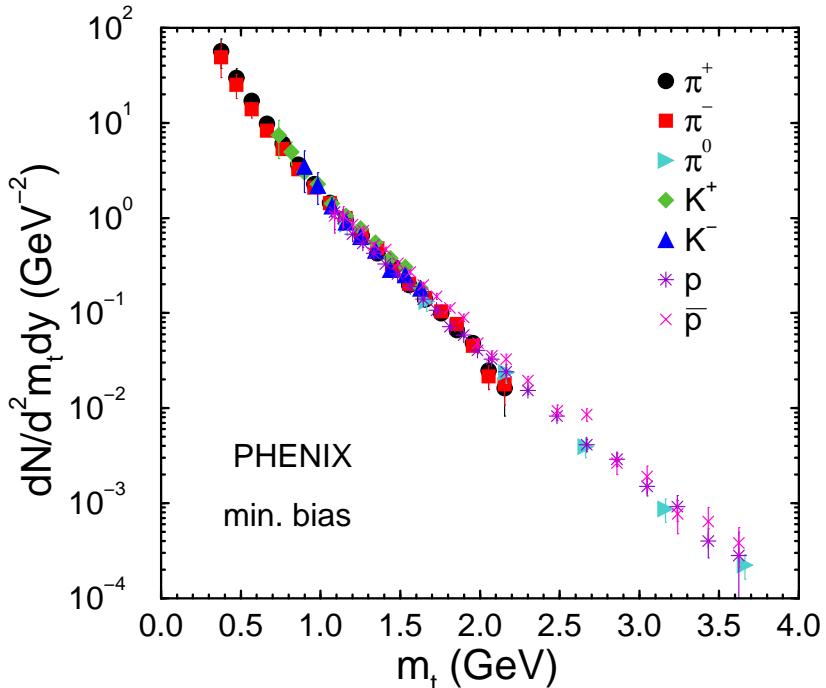


FIG. 2. Transverse mass spectra of figure 1 where the proton and kaon/antikaon data points are multiplied by 1/2 and 2, respectively.

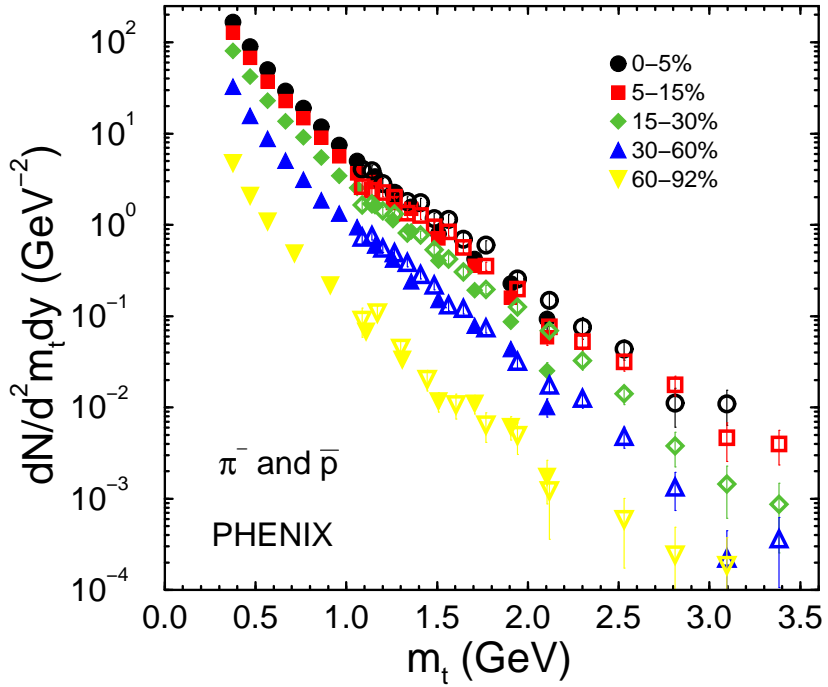


FIG. 3. Transverse mass spectra of π^- and \bar{p} for different centralities at RHIC (data as published in [18]). Filled symbols are for π^- , open symbols for antiprotons.

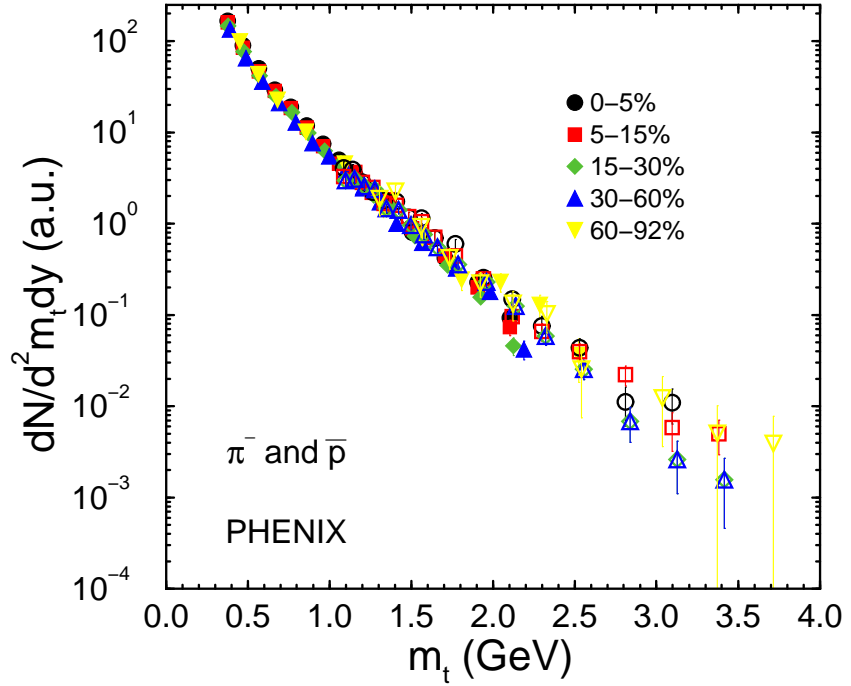


FIG. 4. Rescaled transverse mass spectra of π^- and \bar{p} of the previous figure.

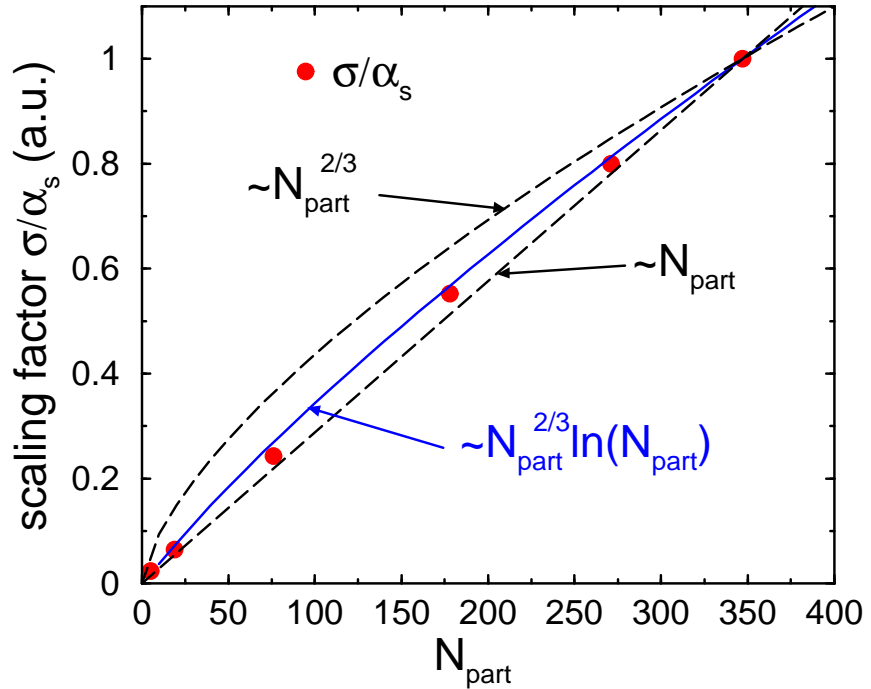


FIG. 5. Scaling factor of the absolute normalization of the transverse mass spectra. All curves are normalized to the most central bin at $N_{\text{part}} = 347$.

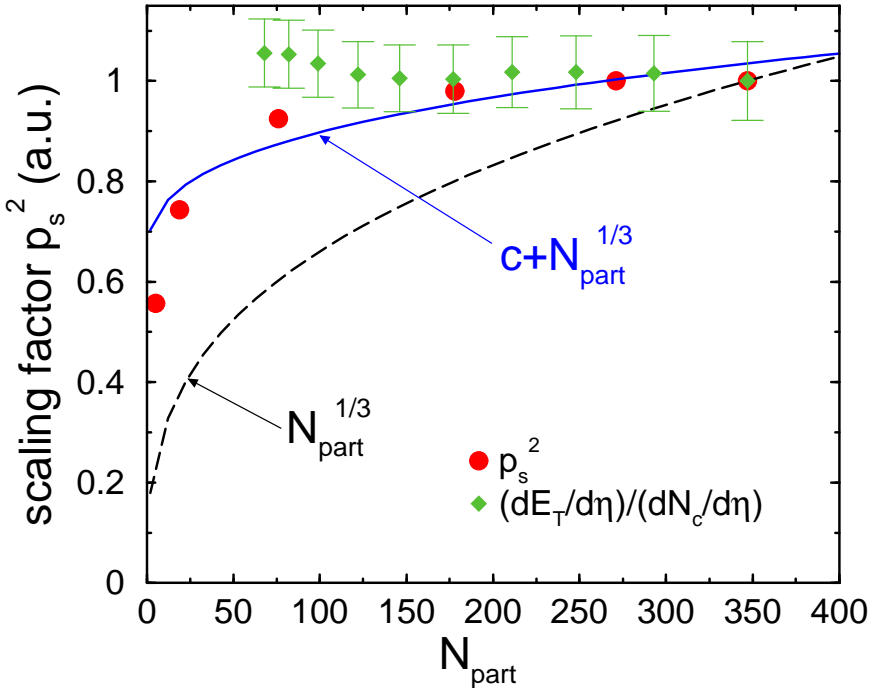


FIG. 6. Momentum scaling factor p_s^2 as extracted from the rescaling of the m_t -spectra. The data for the transverse energy per charged particle from PHENIX [30] is plotted for comparison and normalized to the most central bin.